Inorganic Chemistry

Article

pubs.acs.org/IC

Bioinorganic Chemistry of Parkinson's Disease: Affinity and Structural Features of Cu(I) Binding to the Full-Length β-Synuclein Protein

Marco C. Miotto,[†] Mayra D. Pavese,[†] Liliana Quintanar,[‡] Markus Zweckstetter,[§,∥,⊥] Christian Griesinger,[§] and Claudio O. Fernández*[,†,§]

[†]Max Planck Laboratory for Structural Biology, Chemistry and Molecular Biophysics of Rosario and Instituto de Investigaciones para el Descubrimiento de Fármacos de Rosario, Universidad Nacional de Rosario, Ocampo y Esmeralda, S2002LRK Rosario, Argentina

[‡]Centro de Investigación y de Estudios Avanzados, Av. Instituto Politécnico Nacional 2508, 07360 D.F., México

[§]Department of NMR-based Structural Biology, Max Planck Institute for Biophysical Chemistry, Am Fassberg 11, D-37077 Göttingen, Germany

[∥]Deutches Zentrum für Neurodegenerative Erkrankungen, von-Siebold-Str. 3a, 37075 Göttingen, Germany

[⊥]Department of Neurology, University Medical Center Göttingen, University of Göttingen, Waldweg 33, 37073 Göttingen, Germany

Supporting Information

ABSTRACT: Alterations in the levels of copper in brain tissue and formation of α-synuclein (αS)-copper complexes might play a key role in the amyloid aggregation of αS and the onset of Parkinson's disease (PD). Recently, we demonstrated that formation of the high-affinity Cu(I) complex with the N-terminally acetylated form of the protein αS substantially increases and stabilizes local conformations with α-helical secondary structure and restricted motility. In this work, we performed a detailed NMR-based structural characterization of the Cu(I) complexes with the full-length acetylated form of its homologue β-synuclein (βS), which is colocalized with αS in vivo and can bind copper ions. Our results show that, similarly to αS, the N-terminal region of βS constitutes the preferential binding interface for Cu(I) ions, encompassing two independent and noninteractive Cu(I) binding sites. According to these results, βS binds the metal ion with higher affinity than αS, in a coordination environment that involves the participation of Met-1, Met-5, and Met-10 residues (site 1). Compared to αS, the shift of His from position 50 to 65 in the N-terminal region of βS does not change the Cu(I) affinity features at that site (site 2). Interestingly, the formation of the high-affinity βS−Cu(I) complex at site 1 in the N-terminus promotes a short α-helix conformation that is restricted to the 1−5 segment of the Acβ S sequence, which differs with the substantial increase in α-helix conformations seen for N-terminally acetylated αS upon Cu(I) complexation. Our NMR data demonstrate conclusively that the differences observed in the conformational transitions triggered by Cu(I) binding to AcαS and Acβ S find a correlation at the level of their backbone dynamic properties; added to the potential biological implications of these findings, this fact opens new avenues of investigations into the bioinorganic chemistry of PD.

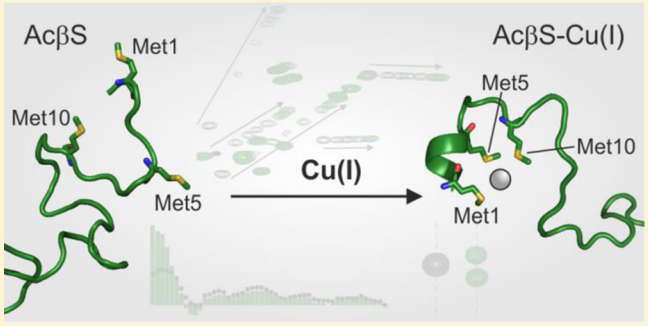

INTRODUCTION

The misfolding and aberrant self-assembly of proteins are considered key molecular events in several neurodegenerative disorders such as Creutzfeldt-Jakob's disease, Alzheimer's (AD), and Parkinson's disease (PD).[1,2] Although these structural transformations have been observed for a range of proteins, the mechanisms behind the self-assembly of proteins into fibrillar deposits remain unknown. An example of these types of proteins is the synuclein family, a group of intrinsically disordered proteins (αS, βS, and γS) that are abundant in the brain and play a causative role in neurodegenerative disorders and cancer.[3] Their physiological roles are poorly understood, though αS is suggested to be implicated in the folding pathways of SNARE proteins.[4−6] However, in disorders such as PD or dementia with Lewy bodies it is well-documented that αS adopts conformations with pronounced β-sheet secondary structure that trigger neurotoxicity and the progressive loss of dopaminergic neuronal cells in the substantia nigra, reflected by the presence of amyloid fibrillar aggregates.[7,8] Interestingly, βS lacks the central hydrophobic cluster in its sequence (Figure 1) and might have a protective role on these events in vitro and in vivo.[9−13] For these reasons, the biological and chemical

Received: May 23, 2017
Published: August 18, 2017

DOI: 10.1021/acs.inorgchem.7b01292
Inorg. Chem. 2017, 56, 10387−10395

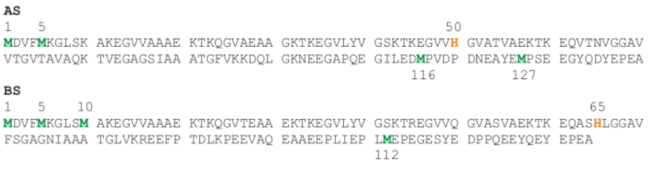

Figure 1. Primary sequence of full-length αS and βS proteins. Met and His residues involved in Cu(I) binding are highlighted.

behaviors of βS have been extensively investigated and compared to αS.[14−21]

Transition-metal ion homeostasis (copper, iron, zinc) plays a key role in neurodegenerative disorders, as these ions are considered one of the possible factors leading to protein aggregation.[22−24] Indeed, metal−protein interactions can have an important impact on the kinetics of amyloid aggregation and the neurotoxicity of protein aggregates; particularly, this has been demonstrated for the case of copper and zinc interactions with the amyloid beta peptide,[25] associated with Alzheimer's disease. Furthermore, coordination environments for copper and zinc complexes in the amyloid beta peptide have been very well-characterized by several biophysical and structural studies, whereas the detailed knowledge of the structural and binding features of these relevant metal ions as well as the mechanism by which the metal ions might participate in the aggregation process have contributed to the design of new therapeutical schemes.[26,27]

An unresolved question in the neuropathology of PD relates to the role of metal ions in αS fibril formation and neurodegeneration. Protein−metal interactions have been demonstrated to play an important role in αS aggregation[23,28] and might represent the link between the pathological processes of protein aggregation, oxidative damage, and neuronal cell loss.[22,24,29] Particularly, the structural and affinity features for the interaction between αS and the Cu(II)/Cu(I) couple became recently the focus of numerous investigations.[15,18,28,30−35] Added to the abundant evidence revealing that αS undergoes N-terminal acetylation in vivo (AcαS),[36,37] it was reported recently that this modification of αS abolishes Cu(II) binding at the high-affinity binding site.[38] Since copper ions are predominantly found in their Cu(I) state in the reducing environment of living cells, characterization of the physiologically relevant AcαS−Cu(I) complexes is particularly important.[34,39] These studies revealed that the Cu(I) binding sites were preserved in the acetylated form of the protein.[34,40,41] From the structural residue-specific characterization of Cu(I) binding to AcαS, it was demonstrated that the protein is able to bind Cu(I) in a coordination environment that involves the participation of Met1 and Met5 as the main anchoring residues.[18,33,34] The formation of an AcαS−Cu(I) complex at the N-terminal region induced a dramatic impact on protein conformation, leading to stabilized local conformations with α-helical secondary structure and restricted motility.[34]

Advances in the bioinorganic chemistry of Parkinson's disease require that details of the binding specificity of Cu(I) to the synuclein family and its conformational consequences to be better understood. To this end, we have previously designed and studied Cu(I) complexes with site-directed mutants of αS.[40] In the present work, we conducted experiments to delineate the Cu(I) binding features of its natural homologue βS. The full-length protein βS constitutes an excellent and natural occurring model to understand and gain details of the specificity, structural, and affinity features behind Cu(I) binding to synucleins, because (1) βS shows a high degree of homology with αS, particularly at the N-terminal region, where cotranslational acetylation and specific Cu(I) binding occurs (Figure 1); (2) the high-affinity Met-Cu(I) binding motif Met^1-X$_n$-Met^5 in αS is replaced by the Met^1-X$_n$-Met^5-X$_n$-Met^{10} sequence, presenting an additional Met residue in the 1−10 segment, (3) the only His residue, located in one of the two regions affected by Cu(I) binding at the N-terminus, is shifted from position 50 in αS to position 65 in βS; (4) βS largely lacks the long-range interactions present in αS, involving N- and C-terminus and non-amyloid-β component and C-terminus contacts, respectively.[14,17] Moreover, both proteins are colocalized at the presynaptic terminals of dopaminergic neurons and are expressed at similar levels,[3,42−44] whereas altered expression levels of both synucleins have been correlated with disease onset,[45] adding biological implications to our investigations.

The structural and dynamical properties of full-length βS and its Cu(II) complexes in solution have been previously elucidated.[14−17] In addition, Cu(I) interactions with βS peptide models containing the N-terminal Met binding site have been reported.[18,46] However, key aspects such as the impact of Cu(I) binding on βS protein conformation and dynamics, the potential role of other Cu(I) anchoring residues in the protein sequence, as well as the quantification of the strength of Cu(I) interaction at these sites remain unknown. Here, we report a detailed structural characterization of the Cu(I) complexes with the full-length, acetylated form of the βS protein. By using an NMR-based approach we identified three Cu(I) sites at the N- and C-terminal region of the βS protein, elucidated their main anchoring residues, and determined their affinity features. A comparative analysis with αS revealed that βS binds this metal ion with higher affinity, involving Met-1, Met-5, and Met-10 residues at the N-terminal region as primary metal-anchoring ligands. Notably, the formation of the high-affinity βS−Cu(I) complex at the N-terminus seems to rely on the induction of a local, subtle structural arrangement that brings the distant Met-10 residue close to the Cu(I) ion (site 1). Compared to αS, the shift of His from position 50 to 65 in the N-terminal region of βS does not change the structural and affinity features of Cu(I) binding at this site (site 2), whereas coordination of Cu(I) to the Met binding site at the C-terminus is strongly reduced due to the lack of one of the anchoring sulfur atoms (Met-116/Met-127 in αS and Met-112 in βS). Our findings demonstrate that the structural consequences derived from the metal−protein interaction in AcβS differ from those observed in AcαS, highlighting their potential implications in biological or pathological processes related to metal transport, membrane binding, and/or protein aggregation.

EXPERIMENTAL SECTION

Protein and Reagents. ^{15}N and ^{15}N−^{13}C isotopically enriched N-terminally acetylated βS (AcβS) was obtained by cotransfecting *Escherichia coli* BL21 cells with the plasmid harboring the wild-type βS gene and a second one that encodes for the components of yeast NatB acetylase complex.[47] Both plasmids carried different antibiotic resistance, namely, Ampicillin and Chloramphenicol, to select the doubly transformed *E. coli* colonies. Purification was performed as previously reported,[48] with the exception that both antibiotics were included in the growth flasks to avoid plasmid purge during growth and expression. The final purity of the AcβS samples was determined by sodium dodecyl sulfate polyacrylamide gel electrophoresis (SDS-PAGE). Copper sulfate, L-ascorbic acid, 2-(*N*-morpholino)-ethanesulfonic acid (MES) buffer, and D_2O were purchased from

DOI: 10.1021/acs.inorgchem.7b01292
Inorg. Chem. 2017, 56, 10387−10395

Merck or Sigma. The chemicals 4,4-dimethyl-4-silapentane-1-sulfonic acid (DSS), ^{15}N NH_4Cl, and U−^{13}C glucose were purchased from Cambridge Isotope Laboratories or Sigma. Purified protein samples were dissolved in 20 mM MES buffer supplemented with 100 mM NaCl at pH 6.5 (Buffer A). Protein concentrations were determined spectrophotometrically by measuring absorption at 274 nm and using an epsilon value of 5600 M^{-1} cm^{-1}. The peptide Ac-^{1}MDVFMKGLSMAKEGV^{15}-amide (1−15 AcβS) was purchased from EZBioLab (purity 96.66%). The absorption extinction coefficient of the peptide was determined using a calibration curve prepared in Buffer A, weighting out the purified dry peptide samples. The absorption extinction coefficient for the peptide was 19 666 cm^{-1} M^{-1} at 214 nm and was used to determine the peptide concentration in each sample.

Generation of Peptide and Protein Cu(I) Complexes. To generate the Cu(I) complexes of the model peptide 1−15 AcβS and full-length AcβS protein, the respective Cu(II) complexes were prepared first and then reduced with ascorbate under anaerobic conditions. In all cases, the final concentration of ascorbate used to generate each Cu(I) complex was 100:1 relative to the amount of added Cu(II). Before and after ascorbate addition, samples were treated with a flow of N_2 during 5 min to generate an N_2 atmosphere. In all cases, NMR tubes sealed under N_2 atmosphere were used, as previously described.[33,40,41]

NMR Experiments. NMR spectra were recorded on a Bruker 600 MHz HD Avance III spectrometer, equipped with a cryogenically cooled triple resonance $^{1}H(^{13}C/^{15}N)$ TCI probe. One-dimensional (1D) ^{1}H experiments, two-dimensional (2D) $^{1}H-^{15}N$ HSQC, ^{15}N R_1/R_2 relaxation rates, $^{1}H-^{15}N$ NOE experiments, HNHA, and triple resonance experiments (HNCACB, HN(CO)CACB, HNCO, and HN(CA)CO) were all recorded in Buffer A at 15 °C using standard pulse sequences from the Topspin suite (Bruker) library. Sequence-specific assignments for the backbone of unbound and Cu(I)-bound AcβS were obtained using the above-mentioned triple resonance experiments. The backbone assignment of acetylated AcβS (Table S1) was deposited at the Biological Magnetic Resonance Data bank under No. 27027. DSS was used for chemical shift referencing. Mean weighted chemical shift differences (mw$\Delta\delta$) were calculated as $[(\Delta\delta^{1}H)^2 + (\Delta\delta^{15}N/10)^2]^{1/2}$.[49] Neighbor-corrected secondary structure propensity (ncSP) scores were calculated using Cα, Cβ, CO, and Hα chemical shifts as input.[50,51] Positive ncSP values ranging from 0 to 1 and negative values from 0 to −1 are indicative of α or β structures, respectively. Three-bond HN-Hα coupling constants ($^{3}J_{HN\text{-}H\alpha}$) were obtained from the ratio between the intensities of the diagonal peaks and cross-peaks in the HNHA experiment.[52] Three-bond HN-Hα coupling constants ($^{3}J_{HN\text{-}H\alpha}$) are sensitive to the torsion angle ϕ populated by each residue in the protein sequence and thus report on secondary structure content. This coupling falls in the range of 3.0−6.0 Hz for an α-helix and 8.0−11.0 Hz for a β-sheet structure. For a random coil, a weighted average of these values is observed that typically ranges between 6.0 and 8.0 Hz for most residues.[53,54] Acquisition and processing of NMR spectra were performed using TOPSPIN 3.1 (Bruker Biospin). 2D spectra analysis and visualization were performed with CCPN. Sequence-specific backbone assignments and $^{3}J_{HN\text{-}H\alpha}$ couplings analysis were done with CARA.[55]

AcβS−Cu(I) Complex Affinities. The affinity features of Cu(I) binding to AcβS and the 1−15 AcβS peptide were determined from 1D ^{1}H NMR and 2D $^{1}H-^{15}N$ HSQC experiments using 20 μM protein and peptide samples recorded at increasing concentrations of the metal ion. Changes in $^{1}H-^{15}N$ mw$\Delta\delta$ values of amide resonances of Asp-2, Met-5, Lys-6, Leu-8, and Ala-11 (site 1) and Lys-60, Ala-63, Ser-64, Gly-68, and Val-70 (site 2) of AcβS were fit to the model incorporating one Cu(I) ion per site using the program DynaFit.[56] This model assumes that the different AcβS sites are independent and that the availability of free Cu(I) for one site at each titration point depends on the amount of metal bound to the others. In the following equations, AcβS species 1 and 2 refer to Cu(I) binding to sites 1 and 2, respectively:

$$Ac\beta S_1 - Cu(I) \leftrightarrow Ac\beta S_1 + Cu(I) \quad K_{d1}$$

$$Ac\beta S_2 - Cu(I) \leftrightarrow Ac\beta S_2 + Cu(I) \quad K_{d2}$$

In the case of the 1−15 AcβS peptide, the Hε protons of Met-1, Met-5, and Met-10, in close proximity to the sulfur atoms coordinating Cu(I) at site 1, were used to estimate the affinity features of the AcβS−Cu(I) complex according to a single-site model:

$$Ac\beta S_1 - Cu(I) \leftrightarrow Ac\beta S_1 + Cu(I) \quad K_{d1}$$

The apparent K_d values estimated from the DynaFit analysis were then corrected to calculate the conditional dissociation constants ($^{c}K_d$; see Supporting Information). In all cases, the K_d values reported in the text correspond to the conditional dissociation constants ($^{c}K_d$).

RESULTS

Binding Sites and Affinity Features of Cu(I) Complexes in AcβS. To identify Cu(I) binding sites in AcβS and determine their affinity features, we used 2D NMR spectroscopy. Upon titration of ^{15}N-enriched AcβS with increasing concentrations of Cu(I), the $^{1}H-^{15}N$ heteronuclear single quantum correlation (HSQC) spectra retained the excellent resolution of the uncomplexed protein but demonstrated large chemical shift changes in a discrete number of amide resonances belonging to the first N-terminal residues, with smaller shift perturbations around His-65 and Met-112 amide groups (Figure 2A,B). The effects on His-65 and Met-112 amide resonances were enhanced in samples containing increasing equivalents of the added metal ion. These results demonstrated that Cu(I) binding to AcβS would be mediated by the following ligand sets: Met-1/Met-5/Met-10, His-65, and Met-112, in which the degree of metal-induced perturbations decreased in the order Met-1/Met-5/Met-10 (site 1) > His-65 (site 2) ≫ Met-112 (site 3).

The estimated affinities for the Cu(I) complexes at the full-length protein confirm this order, with values of $^{c}K_{d1}$ = 0.68 ± 0.07 nM for Cu(I) binding at site 1 and $^{c}K_{d2}$ = 16 ± 5 nM for Cu(I) binding at site 2 (Figure 2C). The Cu(I) complex at the Met-112 (site 3) site was not included in the binding model; however, from the experimental conditions we estimated that $^{c}K_{d3}$ for Cu(I) binding at this site is in the low micromolar range.

To gain further insights into the Cu(I) binding to the high-affinity Met motif, we next performed NMR experiments aimed to monitor the resonances of Met side chains in the full-length protein. To detect the characteristic Hε proton resonances corresponding to the S−CH_3 groups of Met residues we performed 1D ^{1}H NMR experiments. As shown in Figure S1, the presence of Cu(I) ions caused the selective chemical shift changes of Hε resonances in the S−CH_3 groups of Met residues, confirming that Cu(I) binding to the site 1 and site 3 is mediated by coordination of sulfurs atoms from Met-1/Met-5/Met-10 and Met-112, respectively.

According to these results, we then investigated the binding features of Cu(I) ions to the synthetic peptide 1−15 AcβS, containing the Met-1/Met-5/Met-10 binding motif. The binding features of Cu(I) complexed to the synthetic peptide, as monitored by the metal ion-induced effects on the Hε chemical shifts of S−CH_3 Met groups, were similar to those observed for site 1 in the full-length protein (Figure S2A), consistent with the absence of interplay between this site and the other identified Cu(I) binding motifs. The estimated affinity for the Cu(I) complex in the 1−15 AcβS peptide resulted to be $^{c}K_d$ = 0.55 ± 0.10 nM (Figure S2B), in agreement with the value obtained for the high-affinity site 1 in the full-length protein.

DOI: 10.1021/acs.inorgchem.7b01292
Inorg. Chem. 2017, 56, 10387−10395

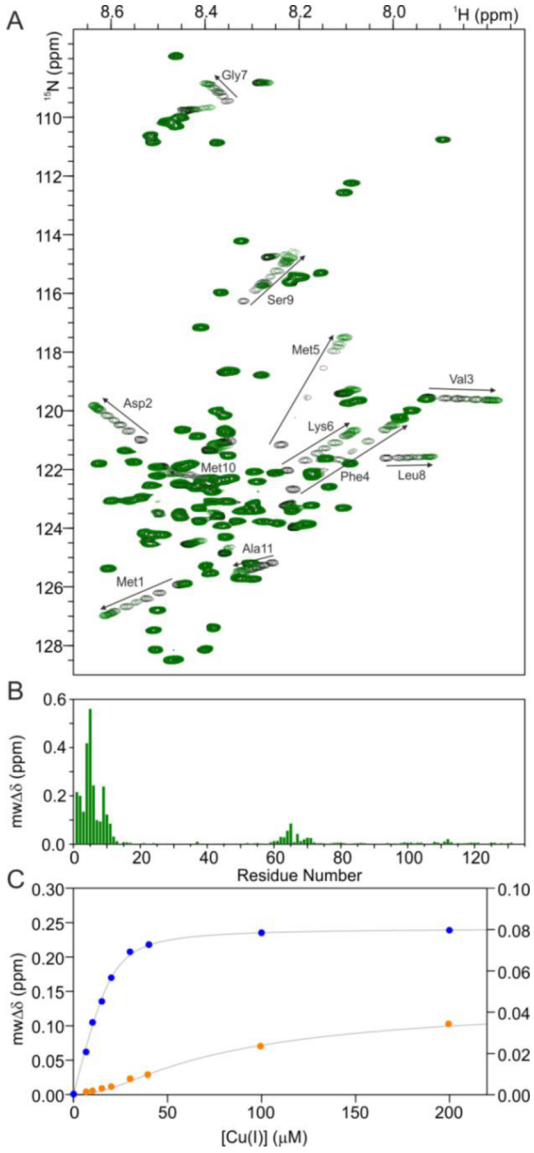

Figure 2. NMR analysis of Cu(I) binding to AcβS. (A) Overlaid ^{1}H−^{15}N HSQC spectra of AcβS in the absence and presence of increasing Cu(I) concentrations. From black to green: 0, 0.25, 0.50, 0.75, 1.0, 1.5, 2.0, 3.0, 5.0, and 10.0 equiv of Cu(I). Most-affected residues are labeled. (B) Differences in the ^{1}H−^{15}N mw$\Delta\delta$ between free and Cu(I)-complexed AcβS at a molar ratio of 10:1. (C) Binding curves of Cu(I) to sites 1 (blue ●) and 2 (orange ●) of AcβS as monitored by the average change in the mw$\Delta\delta$ for ^{1}H and ^{15}N of most affected amide resonances: Asp-2, Met-5, Lys-6, Leu-8, and Ala-11 (site 1) and Lys-60, Ala-63, Ser-64, Gly-68, and Val-70 (site 2). Curves represent the fit to a model incorporating complexes of Cu(I) into two classes of independent, noninteractive binding sites, using the program DynaFit. Experiments were recorded at 15 °C using ^{15}N isotopically enriched AcβS (20 μM) samples dissolved in Buffer A.

Conformation of the Cu(I) Complexed State of AcβS.

The NMR data demonstrated that AcβS is able to interact with Cu(I) with the same binding preferences as the acetylated αS; the N-terminal region constitutes the main anchoring interface for Cu(I) binding. The relative affinities indicates a stronger Cu(I) affinity for AcβS ($^{c}K_{d1}$ = 0.68 ± 0.07 nM) than AcαS ($^{c}K_{d1}$ = 3.9 ± 1.0 nM)[34] at the N-terminal Met binding motif. Since formation of the high-affinity AcαS−Cu(I) complex at the N-terminal region induced a dramatic impact on protein conformation, leading to stabilized local conformations with α-helical secondary structure and restricted motility,[34] our results in AcβS motivated us to evaluate the AcβS−Cu(I) complexes in terms of their conformational properties. NMR chemical shifts are frequently used to probe the propensity of intrinsically disordered proteins to sample different regions of conformational space.[57] We first used ^{13}C-, ^{15}N-, and ^{1}H-based chemical shifts to calculate neighbor-corrected secondary structure propensity scores (ncSP) and compare the secondary structure propensities of AcβS and its Cu(I) complexed form. As shown in Figure 3A, the ncSP profiles for the acetylated metal-free form of the protein showed a small population of α-helix conformation near the N-terminus, limited to the 1−5 segment. Indeed, it is that region that shows the major divergences between the chemical shift data measured for the metal-free and metal-complexed states of AcβS, consistent with an increase in α-helix in the first five residues of Cu(I)-bound AcβS, as

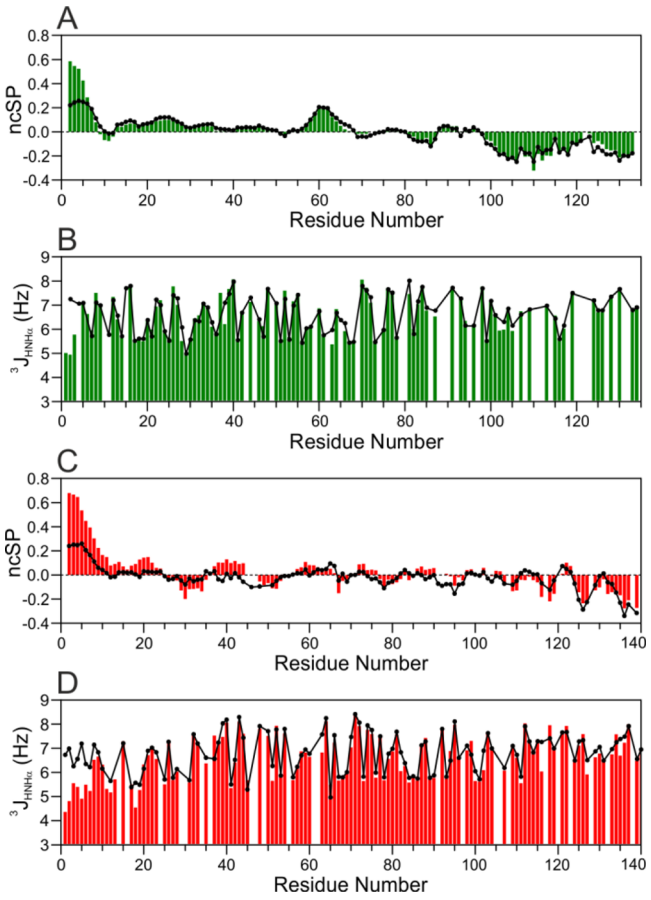

Figure 3. Impact of Cu(I) binding on the structural properties of AcβS. (A) Secondary structure propensity as determined by the measurement of ncSP scores in AcβS (black line) and AcβS−Cu(I) forms (green bars). ^{13}Cα, ^{13}Cβ, ^{13}CO, ^{15}N, and Hα chemical shifts were used to calculate the residue-specific ncSP scores. Positive values ranging from 0 to 1 and negative values from 0 to −1 represent the propensities to α and β structures, respectively. (B) $^{3}J_{HN\text{-}H\alpha}$ couplings measured for AcβS (black line) and AcβS−Cu(I) (green bars). Experiments were recorded at 15 °C using ^{15}N AcβS (200 μM) and ^{13}C, ^{15}N, AcβS (300 μM) samples dissolved in Buffer A, in the absence and presence of 2 equiv of Cu(I). For comparative purposes, (C, D) the ncSP and $^{3}J_{HN\text{-}H\alpha}$ profiles measured for AcαS (black line) and its AcαS−Cu(I) form (red bars), recorded under the same experimental conditions.

DOI: 10.1021/acs.inorgchem.7b01292
Inorg. Chem. 2017, 56, 10387−10395

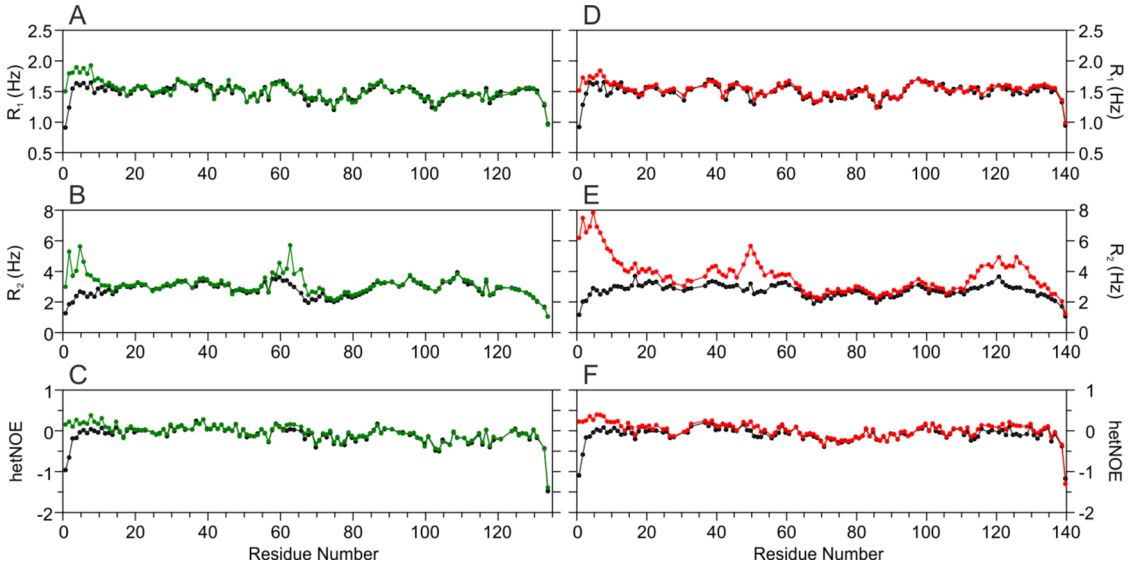

Figure 4. ^{15}N relaxation parameters of AcβS and its Cu(I) complexes. (A) R_1, (B) R_2, and (C) ^{1}H−^{15}N hetNOE relaxation data of AcβS in the absence (black) and presence (green) of Cu(I). Experiments were recorded at 15 °C using ^{15}N isotopically enriched AcβS (200 μM) samples dissolved in Buffer A in the absence and presence of 2 equiv of Cu(I). Panels **D**−**F** show the ^{15}N relaxation parameters of AcαS (black) and its Cu(I) (red) complexes, recorded under the same experimental conditions described for AcβS samples. (B, E) The increase of R_2 values around His 65 in AcβS−Cu(I) and His-50 and Met-116/127 residues in AcαS−Cu(I) reflects the fast exchange of Cu(I) at these secondary sites, as previously reported.[34]

evidenced by the positive deviations in the ncSP values. Next, we measured $^3J_{\text{HN-H}\alpha}$ couplings in both AcβS and AcβS−Cu(I) states, which are reliable quantitative reporters of the time-averaged distribution of the backbone torsion angles ϕ.[54] With the exception of the decrease in $^3J_{\text{HN-H}\alpha}$ observed for residues in the 1−5 segment of AcβS upon Cu(I) binding, the values measured for the two forms of the protein were essentially indistinguishable. Added to the evidence coming from the ncSP scores, the $^3J_{\text{HN-H}\alpha}$ couplings, observed for the residues 1−5 of AcβS in the presence of Cu(I), ranged between 4.8 and 5.8 Hz, indicative of an increased α-helix conformation in the 1−5 segment of AcβS−Cu(I) relative to its metal-free state (Figure 3B).

When compared with the increase in α-helix content in the 1−10 segment of Cu(I)-complexed AcαS (Figure 3C,D), which seems to be followed by a transiently populated helix in the 11−25 region (Figure 3C), the α-helix transition observed for N-terminally acetylated βS upon Cu(I) binding is restricted to the 1−5 segment of the AcβS sequence. Because the amino acid sequence of AcαS and AcβS is identical within the first 10 residues with the exception of Met-10, the more restricted nature of the Cu(I)-induced helix formation might be associated with the metal coordination of Met-10 in AcβS. Metal coordination of Met-10 in AcβS would then require a backbone bend or turn around residues 6−8, leading to a break of the helical architecture at that position of the AcβS sequence.

Dynamic Properties of the Cu(I) Complexed State of AcβS. The structural implications of Cu(I) complexation to AcβS were also evaluated in terms of the dynamic properties of the Cu(I) complexed state of AcβS. To this purpose, we measured ^{15}N R_1 and R_2 relaxation rates and heteronuclear (^{1}H−^{15}N) nuclear Overhauser effects (hetNOEs). This set of experiments was first measured on the free state of AcβS, in which the relaxation parameters showed a similar sequence dependence, with lower values at the termini of the protein and a plateau at the center of the relaxation profile, showing R_1 values between 1.2 and 1.7 s^{-1}, R_2 values between 2.0 and 3.6 s^{-1}, and hetNOEs in the range from −0.5 to 0.1 (Figure 4A−C). Complexation with Cu(I) resulted in a slight increase in the R_1 values for the 1−10 segment of the protein sequence (mean R_1 values of 1.5 and 1.8 s^{-1} in the free and complexed protein, respectively); however, more pronounced deviations were found in the R_2 values (mean R_2 values of 2.2 and 4.0 s^{-1} for the free and complexed protein, respectively) and NOE data (mean hetNOEs values of −0.2 and 0.2 in the free and complexed protein, respectively). These data indicate restricted local sampling in the pico- to nanosecond time scale, and, although in AcβS, complexation with Cu(I) induces a short α-helical structure, which ends around residues Met-5/Lys-6 (Figure 3A,B), the values shown here report on enhanced conformational order for the 1−10 segment of AcβS−Cu(I) relative to the free protein.

For comparative purposes, the backbone dynamic profiles of the Cu(I) complexed state of AcαS measured under the same experimental conditions are shown in Figure 4D−F. The increments observed for R_1, R_2, and hetNOEs parameters at the 1−10 segment of AcαS−Cu(I) reflect a loss of flexibility due to the stabilization of an α-helical structure in this region, whereas the increment in R_2 values in the segment encompassing residues 11−25, which is absent in the AcβS−Cu(I) complex, is indicative of a conformational exchange process, supporting the occurrence of a dynamically and transiently populated α-helix in that region. The comparison clearly shows that the differences observed in the conformational transitions triggered by Cu(I) binding to AcαS and AcβS find a correlation at the level of their backbone dynamic properties.

DISCUSSION

Copper and the proteins αS and βS are highly abundant in synaptic vesicles and synaptosomes, reaching concentrations of ~300 μM[58,59] and ~50 μM,[43] respectively. Added to the evidence that links metal ions with neurodegeneration, the fact that a pool of loosely bound copper ions would exist on those

DOI: 10.1021/acs.inorgchem.7b01292
Inorg. Chem. 2017, 56, 10387−10395

cellular environments[60,61] and might become available for interacting with αS and βS proteins opens the door to address an unresolved issue, as it is the basis of the neuroprotective role proposed for βS in PD. Indeed, free copper levels were found to have increased in the cerebrospinal fluid of PD patients.[62,63] In consequence, in this work we characterized the Cu(I) interaction features of Acβ S and performed a comparative analysis with Acα S. We found that, similarly to Acα S,[34] Acβ S binds Cu(I) at three different sites; our NMR results revealed that these sites are independent and noninteractive, with affinities of $^{c}K_{d1}$ = 0.68 ± 0.07 nM for site 1 (Met-1/Met-5/Met-10), $^{c}K_{d2}$ = 16 ± 5 nM for site 2 (His-65), and in the low micromolar range for site 3 (Met-112). The higher affinity of the Acβ S−Cu(I) complex at site 1 compared to Acα S ($^{c}K_{d1}$ = 3.9. ± 1.0 nM)[34] is supported by the involvement of an extra Met side-chain at position 10, in agreement with results reported for Cu(I) binding to Met motifs in other proteins and peptides.[64,65] By contrast, no differences were observed in the affinity features for Cu(I) interaction centered at His-50 ($^{c}K_{d2}$ = 16 ± 2 nM)[34] and His-65 ($^{c}K_{d2}$ = 16 ± 5 nM) residues in Acα S and Acβ S, respectively.

Previous studies based on transgenic mouse models demonstrated that overexpression of β-synuclein modulates strongly the membrane binding features and the formation of intracellular inclusions of α-synuclein,[11] whereas β-synuclein peptides containing the 1−15 sequence (in which the high-affinity Cu(I) is located) were shown to exert a neuroprotective effect on tissue culture models of α-synucleinopathies.[66] Added to the fact that both synucleins are colocalized, from the biological point of view, our findings allow us to hypothesize that the neuroprotective effect described for Acβ S might be mediated by acting as a Cu(I)-sequestering protein, playing the role of a copper sponge and thereby preventing or attenuating the subsequent oligomerization of Acα S. Interestingly, it was reported that the Metal-Responsive Transcription Factor-1 (MTF-1) efficiently up-regulates the expression of βS, but not that of αS, in the presence of copper,[67] suggesting that βS might act as a metal response factor under normally fluctuating levels of copper in the brain.

Related to this, the design of small molecules that target metal−protein species and regulate metal-induced amyloid aggregation and neurotoxicity is becoming an active area of research.[26,68,69] Interestingly, the precise design of this class of compounds relies on the knowledge of the biological system to be targeted; thus, whereas in AD the efforts are aimed at the Cu(II) and Zn(II)-Aβ peptide interactions, in PD, it is the Acα S−Cu(I) interactions what have become physiologically relevant,[69] since it was reported recently that N-terminal acetylation of αS abolishes Cu(II) binding at the high-affinity Met-1 site present in the nonacetylated protein.[38]

From the structural point of view, the consequences of Cu(I) binding to Acβ S and Acα S differ despite nearly identical amino acid sequences at the N-termini of the two proteins. In Acβ S, complexation with Cu(I) induces a short α-helical structure that ends around residues Met-5/Lys-6. Notably, from the analysis of the NMR landscape for the Cu(I) complexed state of Acβ S, we observed that the signature of the Hα protons of the Gly-7 residue is characterized by the presence of two resonances instead of the expected single, averaged signal observed for these protons in the free Acβ S state or even in the Acα S−Cu(I) complex (Figure S3). This observation is likely the consequence of a structural rearrangement around Gly-7, leading to the formation of a nonhelical compact conformation.[70] Therefore, we suggest that interaction of Met-10 with Cu(I) to form a 3S coordination environment[18] results in the stabilization of a backbone turn around Gly-7. This hypothesis was further supported by the R_1, R_2, and hNOE profiles measured for the Acβ S−Cu(I) complexes, which showed that restrictions to backbone mobility become evident only for the first 10 residues of the protein, consistent with the induction of a short helix-turn conformation in the 1−10 segment of Acβ S upon complexation with Cu(I) (Figure 5A).

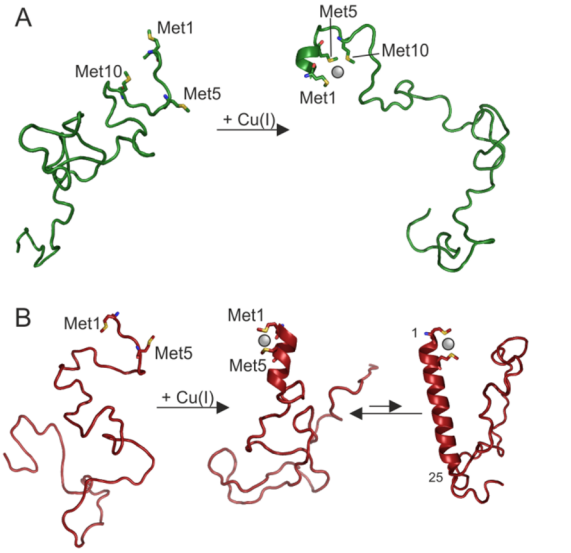

Figure 5. Graphical illustration of conformational and dynamical properties of Acβ S−Cu(I) (A) and Acα S−Cu(I) (B) complexes.

That the N-terminal region constitutes the main anchoring interface for Cu(I) binding to Acβ S, where Cu(I) binds with higher affinity than Acα S at site 1 and without substantial changes at site 2, constitutes relevant conclusions of this study. However, the most important finding of this work is the difference in the nature of the conformational changes observed on synucleins upon Cu(I) binding. In the case of the Acα S variant, Cu(I) interaction with the Met motif at the N-terminus triggers the formation of a stable α-helical structure at the 1−10 segment that seems to be followed by a dynamically and transiently populated helix in the region comprising residues 11 to 25, as concluded by backbone dynamic NMR experiments (Figure 5B). In contrast, for Acβ S, complexation with Cu(I) induces a short α-helical structure that ends around residues Met-5/Lys-6 and would be followed by a backbone bend or turn, leading to a break of the helical architecture at that position of the protein sequence, as reflected by the chemical shift and backbone dynamic NMR profiles. The differences in conformational and dynamical properties observed for Acα S−Cu(I) and Acβ S−Cu(I) complexes might have both physiological and pathological implications, since processes like membrane binding, metal transport, or protein amyloid aggregation constitute molecular events, where helical secondary structure elements have been reported to play a major role.[71−74] At this juncture, combined efforts from the fields of structural, cellular, and animal biology will be critical to address such important, unresolved issues and support the notion of PD as a metal-associated neurodegenerative disorder.

DOI: 10.1021/acs.inorgchem.7b01292
Inorg. Chem. 2017, 56, 10387−10395

■ ASSOCIATED CONTENT

Supporting Information

The Supporting Information is available free of charge on the ACS Publications website at DOI: 10.1021/acs.inorgchem.7b01292.

Calculation of the conditional dissociation constants ($^{c}K_{d}$) values; NMR ^{1}H spectra of Cu(I) titration to the AcβS protein; NMR ^{1}H spectra and binding curve of Cu(I) titration to the 1−15 AcβS peptide; HN-Hα strips of the HNHA experiment corresponding to Gly-7 resonance in AcβS and AcβS−Cu(I); and table of ^{13}Cα, ^{13}Cβ, ^{13}CO, ^{15}N, and ^{1}H^{N} chemical shift assignments measured for AcβS, as deposited at the Biological Magnetic Resonance Data bank under No. 27027 (PDF)

■ AUTHOR INFORMATION

Corresponding Author

*Phone: ++54 341 4237868 (ext. 752). E-mail: fernandez@iidefar-conicet.gob.ar or cfernan@gwdg.de.

ORCID

Marco C. Miotto: 0000-0001-8851-4863

Liliana Quintanar: 0000-0003-3090-7175

Claudio O. Fernández: 0000-0003-0454-7735

Notes

The authors declare no competing financial interest.

■ ACKNOWLEDGMENTS

C.O.F. thanks Universidad Nacional de Rosario (CUA-DAHZ 007/11), ANPCyT-FONCyT (PICT 2014-3704), and the Alexander von Humboldt Foundation (P4507) for financial support. C.O.F. and C.G. thank the Max Planck Society (P10390) for support. L.Q. acknowledges support from Conacyt Grant No. 221134.

■ REFERENCES

(1) Dobson, C. M. Principles of protein folding, misfolding and aggregation. *Semin. Cell Dev. Biol.* **2004**, *15*, 3−16.

(2) Chiti, F.; Dobson, C. M. Protein misfolding, functional amyloid, and human disease. *Annu. Rev. Biochem.* **2006**, *75*, 333−366.

(3) Clayton, D. F.; George, J. M. The synucleins: a family of proteins involved in synaptic function, plasticity, neurodegeneration and disease. *Trends Neurosci.* **1998**, *21*, 249−254.

(4) Chandra, S.; Gallardo, G.; Fernández-Chacón, R.; Schlüter, O. M.; Südhof, T. C. Alpha-synuclein cooperates with CSPalpha in preventing neurodegeneration. *Cell* **2005**, *123*, 383−396.

(5) Choi, B. K.; Choi, M.-G.; Kim, J. Y.; Yang, Y.; Lai, Y.; Kweon, D. H.; Lee, N. K.; Shin, Y. K. Large α-synuclein oligomers inhibit neuronal SNARE-mediated vesicle docking. *Proc. Natl. Acad. Sci. U. S. A.* **2013**, *110*, 4087−4092.

(6) Burré, J.; Sharma, M.; Südhof, T. C. α-Synuclein assembles into higher-order multimers upon membrane binding to promote SNARE complex formation. *Proc. Natl. Acad. Sci. U. S. A.* **2014**, *111*, E4274−E4283.

(7) Spillantini, M. G.; Schmidt, M. L.; Lee, V. M.; Trojanowski, J. Q.; Jakes, R.; Goedert, M. Alpha-synuclein in Lewy bodies. *Nature* **1997**, *388*, 839−840.

(8) Volles, M. J.; Lansbury, P. T. Zeroing in on the pathogenic form of alpha-synuclein and its mechanism of neurotoxicity in Parkinson's disease. *Biochemistry* **2003**, *42*, 7871−7878.

(9) Uversky, V. N.; Li, J.; Souillac, P.; Millett, I. S.; Doniach, S.; Jakes, R.; Goedert, M.; Fink, A. L. Biophysical properties of the synucleins and their propensities to fibrillate: inhibition of alpha-synuclein assembly by beta- and gamma-synucleins. *J. Biol. Chem.* **2002**, *277*, 11970−11978.

(10) Hashimoto, M.; Rockenstein, E.; Mante, M.; Mallory, M.; Masliah, E. beta-Synuclein inhibits alpha-synuclein aggregation: a possible role as an anti-parkinsonian factor. *Neuron* **2001**, *32*, 213−223.

(11) Hashimoto, M.; Rockenstein, E.; Mante, M.; Crews, L.; Bar-On, P.; Gage, F. H.; Marr, R.; Masliah, E. An antiaggregation gene therapy strategy for Lewy body disease utilizing beta-synuclein lentivirus in a transgenic model. *Gene Ther.* **2004**, *11*, 1713−1723.

(12) Rockenstein, E.; Hansen, L. A.; Mallory, M.; Trojanowski, J. Q.; Galasko, D.; Masliah, E. Altered expression of the synuclein family mRNA in Lewy body and Alzheimer's disease. *Brain Res.* **2001**, *914*, 48−56.

(13) Park, J. Y.; Lansbury, P. T. Beta-synuclein inhibits formation of alpha-synuclein protofibrils: a possible therapeutic strategy against Parkinson's disease. *Biochemistry* **2003**, *42*, 3696−3700.

(14) Bertoncini, C. W.; Rasia, R. M.; Lamberto, G. R.; Binolfi, A.; Zweckstetter, M.; Griesinger, C.; Fernandez, C. O. Structural characterization of the intrinsically unfolded protein beta-synuclein, a natural negative regulator of alpha-synuclein aggregation. *J. Mol. Biol.* **2007**, *372*, 708−722.

(15) Binolfi, A.; Lamberto, G. R.; Duran, R.; Quintanar, L.; Bertoncini, C. W.; Souza, J. M.; Cerveñansky, C.; Zweckstetter, M.; Griesinger, C.; Fernández, C. O. Site-specific interactions of Cu(II) with alpha and beta-synuclein: bridging the molecular gap between metal binding and aggregation. *J. Am. Chem. Soc.* **2008**, *130*, 11801−11812.

(16) Sung, Y. H.; Eliezer, D. Secondary structure and dynamics of micelle bound beta- and gamma-synuclein. *Protein Sci.* **2006**, *15*, 1162−1174.

(17) Sung, Y. H.; Eliezer, D. Residual structure, backbone dynamics, and interactions within the synuclein family. *J. Mol. Biol.* **2007**, *372*, 689−707.

(18) De Ricco, R.; Valensin, D.; Dell'Acqua, S.; Casella, L.; Gaggelli, E.; Valensin, G.; Bubacco, L.; Mangani, S. Differences in the binding of copper(I) to α- and β-synuclein. *Inorg. Chem.* **2015**, *54*, 265−272.

(19) Brown, J. W. P.; Buell, A. K.; Michaels, T. C. T.; Meisl, G.; Carozza, J.; Flagmeier, P.; Vendruscolo, M.; Knowles, T. P. J.; Dobson, C. M.; Galvagnion, C. β-Synuclein suppresses both the initiation and amplification steps of α-synuclein aggregation via competitive binding to surfaces. *Sci. Rep.* **2016**, *6*, 36010.

(20) Taschenberger, G.; Toloe, J.; Tereshchenko, J.; Akerboom, J.; Wales, P.; Benz, R.; Becker, S.; Outeiro, T. F.; Looger, L. L.; Bähr, M.; Zweckstetter, M.; Kügler, S. β-synuclein aggregates and induces neurodegeneration in dopaminergic neurons. *Ann. Neurol.* **2013**, *74*, 109−118.

(21) Tenreiro, S.; Rosado-Ramos, R.; Gerhardt, E.; Favretto, F.; Magalhães, F.; Popova, B.; Becker, S.; Zweckstetter, M.; Braus, G. H.; Outeiro, T. F. Yeast reveals similar molecular mechanisms underlying alpha- and beta-synuclein toxicity. *Hum. Mol. Genet.* **2016**, *25*, 275−290.

(22) Brown, D. R. Metals in neurodegenerative disease. *Metallomics* **2011**, *3*, 226−228.

(23) Binolfi, A.; Quintanar, L.; Bertoncini, C. W.; Griesinger, C.; Fernández, C. O. Bioinorganic chemistry of copper coordination to alpha-synuclein: Relevance to Parkinson's disease. *Coord. Chem. Rev.* **2012**, *256*, 2188−2201.

(24) Gaggelli, E.; Kozlowski, H.; Valensin, D.; Valensin, G. Copper homeostasis and neurodegenerative disorders (Alzheimer's, prion, and Parkinson's diseases and amyotrophic lateral sclerosis). *Chem. Rev.* **2006**, *106*, 1995−2044.

(25) DeToma, A. S.; Salamekh, S.; Ramamoorthy, A.; Lim, M. H. Misfolded proteins in Alzheimer's disease and type II diabetes. *Chem. Soc. Rev.* **2012**, *41*, 608−621.

(26) Choi, J. S.; Braymer, J. J.; Nanga, R. P. R.; Ramamoorthy, A.; Lim, M. H. Design of small molecules that target metal-Aβ species and regulate metal-induced Aβ aggregation and neurotoxicity. *Proc. Natl. Acad. Sci. U. S. A.* **2010**, *107*, 21990−21995.

(27) Savelieff, M. G.; DeToma, A. S.; Derrick, J. S.; Lim, M. H. The ongoing search for small molecules to study metal-associated amyloid-β species in Alzheimer's disease. *Acc. Chem. Res.* **2014**, *47*, 2475−2482.
(28) Binolfi, A.; Rodriguez, E. E.; Valensin, D.; D'Amelio, N.; Ippoliti, E.; Obal, G.; Duran, R.; Magistrato, A.; Pritsch, O.; Zweckstetter, M.; Valensin, G.; Carloni, P.; Quintanar, L.; Griesinger, C.; Fernández, C. O. Bioinorganic chemistry of Parkinson's disease: structural determinants for the copper-mediated amyloid formation of alpha-synuclein. *Inorg. Chem.* **2010**, *49*, 10668−10679.
(29) Bolognin, S.; Messori, L.; Zatta, P. Metal ion physiopathology in neurodegenerative disorders. *NeuroMol. Med.* **2009**, *11*, 223−238.
(30) Binolfi, A.; Rasia, R. M.; Bertoncini, C. W.; Ceolin, M.; Zweckstetter, M.; Griesinger, C.; Jovin, T. M.; Fernández, C. O. Interaction of alpha-synuclein with divalent metal ions reveals key differences: a link between structure, binding specificity and fibrillation enhancement. *J. Am. Chem. Soc.* **2006**, *128*, 9893−9901.
(31) Drew, S. C.; Ling Leong, S.; Pham, C. L. L.; Tew, D. J.; Masters, C. L.; Miles, L. A.; Cappai, R.; Barnham, K. J. Cu2+ binding modes of recombinant alpha-synuclein–insights from EPR spectroscopy. *J. Am. Chem. Soc.* **2008**, *130*, 7766−7773.
(32) Lee, J. C.; Gray, H. B.; Winkler, J. R. Copper(II) binding to alpha-synuclein, the Parkinson's protein. *J. Am. Chem. Soc.* **2008**, *130*, 6898−6899.
(33) Binolfi, A.; Valiente-Gabioud, A. A.; Duran, R.; Zweckstetter, M.; Griesinger, C.; Fernandez, C. O. Exploring the structural details of Cu(I) binding to α-synuclein by NMR spectroscopy. *J. Am. Chem. Soc.* **2011**, *133*, 194−196.
(34) Miotto, M. C.; Valiente-Gabioud, A. A.; Rossetti, G.; Zweckstetter, M.; Carloni, P.; Selenko, P.; Griesinger, C.; Binolfi, A.; Fernández, C. O. Copper binding to the N-terminally acetylated, naturally occurring form of alpha-synuclein induces local helical folding. *J. Am. Chem. Soc.* **2015**, *137*, 6444−6447.
(35) Camponeschi, F.; Valensin, D.; Tessari, I.; Bubacco, L.; Dell'Acqua, S.; Casella, L.; Monzani, E.; Gaggelli, E.; Valensin, G. Copper(I)-α-synuclein interaction: structural description of two independent and competing metal binding sites. *Inorg. Chem.* **2013**, *52*, 1358−1367.
(36) Bartels, T.; Choi, J. G.; Selkoe, D. J. α-Synuclein occurs physiologically as a helically folded tetramer that resists aggregation. *Nature* **2011**, *477*, 107−110.
(37) Fauvet, B.; Fares, M.-B.; Samuel, F.; Dikiy, I.; Tandon, A.; Eliezer, D.; Lashuel, H. A. Characterization of semisynthetic and naturally Nα-acetylated α-synuclein in vitro and in intact cells: implications for aggregation and cellular properties of α-synuclein. *J. Biol. Chem.* **2012**, *287*, 28243−28262.
(38) Moriarty, G. M.; Minetti, C. A. S. A.; Remeta, D. P.; Baum, J. A Revised Picture of the Cu(II)−α-Synuclein Complex: The Role of N-Terminal Acetylation. *Biochemistry* **2014**, *53*, 2815−2817.
(39) Dell'Acqua, S.; Pirota, V.; Monzani, E.; Camponeschi, F.; De Ricco, R.; Valensin, D.; Casella, L. Copper(I) Forms a Redox-Stable 1:2 Complex with α-Synuclein N-Terminal Peptide in a Membrane-Like Environment. *Inorg. Chem.* **2016**, *55*, 6100−6106.
(40) Miotto, M. C.; Binolfi, A.; Zweckstetter, M.; Griesinger, C.; Fernández, C. O. Bioinorganic chemistry of synucleinopathies: deciphering the binding features of Met motifs and His-50 in AS-Cu(I) interactions. *J. Inorg. Biochem.* **2014**, *141*, 208−211.
(41) Miotto, M. C.; Rodriguez, E. E.; Valiente-Gabioud, A. A.; Torres-Monserrat, V.; Binolfi, A.; Quintanar, L.; Zweckstetter, M.; Griesinger, C.; Fernández, C. O. Site-Specific Copper-Catalyzed Oxidation of α-Synuclein: Tightening the Link between Metal Binding and Protein Oxidative Damage in Parkinson's Disease. *Inorg. Chem.* **2014**, *53*, 4350−4358.
(42) Maroteaux, L.; Campanelli, J. T.; Scheller, R. H. Synuclein: a neuron-specific protein localized to the nucleus and presynaptic nerve terminal. *J. Neurosci.* **1988**, *8*, 2804−2815.
(43) Wilhelm, B. G.; Mandad, S.; Truckenbrodt, S.; Kröhnert, K.; Schäfer, C.; Rammner, B.; Koo, S. J.; Claßen, G. A.; Krauss, M.; Haucke, V.; Urlaub, H.; Rizzoli, S. O. Composition of isolated synaptic boutons reveals the amounts of vesicle trafficking proteins. *Science* **2014**, *344*, 1023−1028.
(44) Jakes, R.; Spillantini, M. G.; Goedert, M. Identification of two distinct synucleins from human brain. *FEBS Lett.* **1994**, *345*, 27−32.
(45) Wright, J. A.; McHugh, P. C.; Pan, S.; Cunningham, A.; Brown, D. R. Counter-regulation of alpha- and beta-synuclein expression at the transcriptional level. *Mol. Cell. Neurosci.* **2013**, *57*, 33−41.
(46) De Ricco, R.; Valensin, D.; Dell'Acqua, S.; Casella, L.; Hureau, C.; Faller, P. Copper(I/II), α/β-Synuclein and Amyloid-β: Menage à Trois? *ChemBioChem* **2015**, *16*, 2319−2328.
(47) Johnson, M.; Geeves, M. A.; Mulvihill, D. P. Production of amino-terminally acetylated recombinant proteins in E. coli. *Methods Mol. Biol.* **2013**, *981*, 193−200.
(48) Hoyer, W.; Cherny, D.; Subramaniam, V.; Jovin, T. M. Impact of the acidic C-terminal region comprising amino acids 109−140 on alpha-synuclein aggregation in vitro. *Biochemistry* **2004**, *43*, 16233−16242.
(49) Cavanagh, J.; Fairbrother, W. J.; Palmer, A.; Rance, M.; Skelton, N. J. *Protein NMR Spectroscopy;* Academic Press: Amsterdam, Netherlands, 2007.
(50) Marsh, J. A.; Singh, V. K.; Jia, Z.; Forman-Kay, J. D. Sensitivity of secondary structure propensities to sequence differences between alpha- and gamma-synuclein: implications for fibrillation. *Protein Sci.* **2006**, *15*, 2795−2804.
(51) Tamiola, K.; Mulder, F. A. A. Using NMR chemical shifts to calculate the propensity for structural order and disorder in proteins. *Biochem. Soc. Trans.* **2012**, *40*, 1014−1020.
(52) Vuister, G. W.; Bax, A. Quantitative J correlation: a new approach for measuring homonuclear three-bond J(HNH.alpha.) coupling constants in 15N-enriched proteins. *J. Am. Chem. Soc.* **1993**, *115*, 7772−7777.
(53) Hill, R. B.; Flanagan, J. M.; Prestegard, J. H. 1H and 15N magnetic resonance assignments, secondary structure, and tertiary fold of Escherichia coli DnaJ(1−78). *Biochemistry* **1995**, *34*, 5587−5596.
(54) Serrano, L. Comparison between the phi distribution of the amino acids in the protein database and NMR data indicates that amino acids have various phi propensities in the random coil conformation. *J. Mol. Biol.* **1995**, *254*, 322−333.
(55) Keller, R. L. J. *The Computer Aided Resonance Assignment Tutorial;* Cantina Verlag: Goldau, Switzerland, 2004.
(56) Kuzmic, P. Program DYNAFIT for the analysis of enzyme kinetic data: application to HIV proteinase. *Anal. Biochem.* **1996**, *237*, 260−273.
(57) Wishart, D. S.; Sykes, B. D. Chemical shifts as a tool for structure determination. *Methods Enzymol.* **1994**, *239*, 363−392.
(58) Hopt, A.; Korte, S.; Fink, H.; Panne, U.; Niessner, R.; Jahn, R.; Kretzschmar, H.; Herms, J. Methods for studying synaptosomal copper release. *J. Neurosci. Methods* **2003**, *128*, 159−172.
(59) Scheiber, I. F.; Mercer, J. F.; Dringen, R. Metabolism and functions of copper in brain. *Prog. Neurobiol.* **2014**, *116*, 33−57.
(60) Yang, L.; McRae, R.; Henary, M. M.; Patel, R.; Lai, B.; Vogt, S.; Fahrni, C. J. Imaging of the intracellular topography of copper with a fluorescent sensor and by synchrotron x-ray fluorescence microscopy. *Proc. Natl. Acad. Sci. U. S. A.* **2005**, *102*, 11179−11184.
(61) Schlief, M. L.; Gitlin, J. D. Copper homeostasis in the CNS: a novel link between the NMDA receptor and copper homeostasis in the hippocampus. *Mol. Neurobiol.* **2006**, *33*, 81−90.
(62) Pall, H. S.; Williams, A. C.; Blake, D. R.; Lunec, J.; Gutteridge, J. M.; Hall, M.; Taylor, A. Raised cerebrospinal-fluid copper concentration in Parkinson's disease. *Lancet* **1987**, *330*, 238−241.
(63) Hozumi, I.; Hasegawa, T.; Honda, A.; Ozawa, K.; Hayashi, Y.; Hashimoto, K.; Yamada, M.; Koumura, A.; Sakurai, T.; Kimura, A.; Tanaka, Y.; Satoh, M.; Inuzuka, T. Patterns of levels of biological metals in CSF differ among neurodegenerative diseases. *J. Neurol. Sci.* **2011**, *303*, 95−99.
(64) Jiang, J.; Nadas, I. A.; Kim, M. A.; Franz, K. J. A Mets motif peptide found in copper transport proteins selectively binds Cu(I) with methionine-only coordination. *Inorg. Chem.* **2005**, *44*, 9787−9794.

DOI: 10.1021/acs.inorgchem.7b01292
Inorg. Chem. 2017, 56, 10387−10395

(65) Rubino, J. T.; Riggs-Gelasco, P.; Franz, K. J. Methionine motifs of copper transport proteins provide general and flexible thioether-only binding sites for Cu(I) and Ag(I). *JBIC, J. Biol. Inorg. Chem.* **2010**, *15*, 1033−1049.
(66) Windisch, M.; Hutter-Paier, B.; Rockenstein, E.; Hashimoto, M.; Mallory, M.; Masliah, E. Development of a new treatment for Alzheimer's disease and Parkinson's disease using anti-aggregatory beta-synuclein-derived peptides. *J. Mol. Neurosci.* **2002**, *19*, 63−69.
(67) McHugh, P. C.; Wright, J. A.; Brown, D. R. Transcriptional regulation of the beta-synuclein 5′-promoter metal response element by metal transcription factor-1. *PLoS One* **2011**, *6*, e17354.
(68) Hauser-Davis, R. A.; de Freitas, L. V.; Cukierman, D. S.; Cruz, W. S.; Miotto, M. C.; Landeira-Fernandez, J.; Valiente-Gabioud, A. A.; Fernández, C. O.; Rey, N. A. Disruption of zinc and copper interactions with Aβ(1−40) by a non-toxic, isoniazid-derived, hydrazone: a novel biometal homeostasis restoring agent in Alzheimer's disease therapy? *Metallomics* **2015**, *7*, 743−747.
(69) Cukierman, D. S.; Pinheiro, A. B.; Castiñeiras-Filho, S. L. P.; da Silva, A. S. P.; Miotto, M. C.; De Falco, A.; de P Ribeiro, T.; Maisonette, S.; da Cunha, A. L. M. C.; Hauser-Davis, R. A.; Landeira-Fernandez, J.; Aucélio, R. Q.; Outeiro, T. F.; Pereira, M. D.; Fernández, C. O.; Rey, N. A. A moderate metal-binding hydrazone meets the criteria for a bioinorganic approach towards Parkinson's disease: Therapeutic potential, blood-brain barrier crossing evaluation and preliminary toxicological studies. *J. Inorg. Biochem.* **2017**, *170*, 160−168.
(70) Osapay, K.; Case, D. A. Analysis of proton chemical shifts in regular secondary structure of proteins. *J. Biomol. NMR* **1994**, *4*, 215−230.
(71) Anderson, V. L.; Ramlall, T. F.; Rospigliosi, C. C.; Webb, W. W.; Eliezer, D. Identification of a helical intermediate in trifluoroethanol-induced alpha-synuclein aggregation. *Proc. Natl. Acad. Sci. U. S. A.* **2010**, *107*, 18850−18855.
(72) Maltsev, A. S.; Ying, J.; Bax, A. Impact of N-terminal acetylation of α-synuclein on its random coil and lipid binding properties. *Biochemistry* **2012**, *51*, 5004−5013.
(73) Alderson, T. R.; Markley, J. L. Biophysical characterization of α-synuclein and its controversial structure. *Intrinsically Disord. Proteins* **2013**, *1*, 18−39.
(74) Ghosh, D.; Singh, P. K.; Sahay, S.; Jha, N. N.; Jacob, R. S.; Sen, S.; Kumar, A.; Riek, R.; Maji, S. K. Structure based aggregation studies reveal the presence of helix-rich intermediate during α-Synuclein aggregation. *Sci. Rep.* **2015**, *5*, 9228.

DOI: 10.1021/acs.inorgchem.7b01292
Inorg. Chem. 2017, 56, 10387−10395